Research Article

Journal of Environmental Nanotechnology

Thermal Augmentation of Double-tube Heat Exchangers Using Tailored Al_2O_3 Nanoparticle Suspensions

Balla Srinivas[1*], A. V. N. L. Sharma[1] and A. Gopichand[2]

[1]Department of Mechanical Engineering, Gandhi Institute of Engineering and Technology University, Gunupur, OD, India
[2]Department of Mechanical Engineering, Swarnandhra College of Engineering and Technology, Narsapur, AP, India
Received: 25.01.2026 Accepted: 15.02.2026 Published: 30.03.2026
*balla.srinivas@giet.edu

ABSTRACT

This study investigates the thermal–hydraulic performance of a counter-flow double-tube heat exchanger employing Al_2O_3–water nanofluids at varying nanoparticle volume concentrations (0.01%, 0.1%, 0.2%, and 0.3%) and compares their performance with that of the base fluid (water). Experiments were conducted over a mass flow rate range of 0.012–0.026 kg/s to evaluate the influence of nanoparticle concentration and flow rate on key thermal and hydraulic parameters, including Reynolds number (Re), logarithmic mean temperature difference (LMTD), overall heat transfer coefficient (OHTC), number of transfer units (NTU), friction factor, effectiveness, and convective heat transfer coefficient (CHTC). The results revealed that increasing nanoparticle concentration enhances the heat transfer characteristics of the system while inducing only a minor rise in flow resistance. The Reynolds number decreases slightly with nanoparticle addition due to increased viscosity, whereas the OHTC and CHTC show significant improvements up to 30–35% at a concentration of 0.3 vol.%. The NTU and effectiveness also increase, indicating enhanced heat exchange performance. Although a small increase in friction factor was observed, the gain in thermal efficiency far outweighs the hydraulic penalty. Overall, the findings demonstrate that Al_2O_3–water nanofluids are an effective working medium for enhancing the energy efficiency and compactness of double-tube heat exchangers used in cooling, thermal management, and sustainable energy systems.

Keywords: Al_2O_3 nanofluid; Double-tube heat exchanger; Thermal performance; OHTC; NTU; Friction factor; Mass flow rate; Energy efficiency enhancement.

1. INTRODUCTION

Efficient heat transfer is essential in modern thermal systems, including power generation, air conditioning, refrigeration, and renewable energy conversion. With increasing energy demand and the continuous trend toward system miniaturization, improving heat exchange efficiency has become critical for achieving higher performance and sustainability. Conventional heat transfer fluids, including water, ethylene glycol, and mineral oils, exhibit relatively low thermal conductivity (typically below 0.6 W/m·K), which limits their ability to effectively remove or dissipate heat (Ajeeb *et al*. 2023). This limitation often necessitates larger heat exchanger surfaces or higher pumping power, resulting in increased energy consumption and operating costs. To address these challenges, nanofluids, engineered colloidal suspensions of nanosized solid particles (1–100 nm) dispersed in a base fluid, were introduced by Choi and Eastman in 1995 (Aldbea *et al.* 2025). Numerous studies have demonstrated that the inclusion of nanoparticles significantly enhances the thermal and physical properties of conventional fluids, particularly their effective thermal conductivity and convective heat transfer coefficient (Ayoob *et al*. 2025; Bashtani *et al.* 2021). These enhancements are generally attributed to improved effective thermal conductivity, intensified energy transport at the solid–liquid interface, and disruption of the thermal boundary layer. Over the past two decades, nanofluids have shown considerable potential for improving heat transfer performance across a wide range of industrial and energy systems (Choi, 1995; Das *et al.* 2023).

Among the various nanoparticles investigated, aluminium oxide (Al_2O_3) has emerged as one of the most widely studied materials due to its favorable combination of properties, including moderate cost, chemical stability, high melting point, and reasonable thermal conductivity (~36 W/m·K) (Ghazanfari *et al*. 2022; Ghazanfari *et al.* 2023; Gkountas *et al.* 2021). Al_2O_3–water nanofluids have been reported to exhibit 15–40% enhancement in thermal conductivity even at low volume concentrations (<1%) (Issa *et al.* 2021; Kumar *et al.* 2022; Mohammed *et al.* 2012). In addition, Al_2O_3 nanoparticles show good dispersion stability in polar fluids such as water, making

them suitable for practical applications in compact heat exchangers, automotive cooling systems, and electronic thermal management (Murthy *et al.* 2022). However, the improved heat transfer capability is often accompanied by increased viscosity and pressure drop, which can raise pumping power requirements and reduce overall system efficiency (Nam *et al.* 2023). Consequently, a simultaneous evaluation of thermal enhancement and hydraulic penalty is essential for determining optimal operating conditions.

Despite extensive experimental research on Al_2O_3–water nanofluids, most existing studies focus on isolated heat transfer metrics such as the Nusselt number or convective heat transfer coefficient and are often limited to narrow nanoparticle concentration ranges or single flow conditions. Comprehensive experimental investigations that simultaneously evaluate thermal performance (OHTC, CHTC), heat exchanger effectiveness (NTU, effectiveness), and hydraulic penalties (friction factor) under varying mass flow rates in counter-flow double-tube heat exchangers remain scarce. This lack of integrated thermal–hydraulic assessment limits the practical optimization and real-world application of nanofluids in compact and energy-efficient heat exchanger systems. Double-tube heat exchangers (DTHEs) are commonly employed for experimental investigations owing to their simple geometry, well-defined flow characteristics, and ease of instrumentation. Several studies have reported improved heat transfer coefficients and Nusselt numbers when nanofluids are used in double-pipe or helical heat exchangers (Patil *et al.* 2025). For instance, (Rashid *et al.* 2025) comprehensively reviewed recent advances in nanofluid-assisted double-pipe heat exchangers (DPHEs) and reported that nanofluid addition significantly improves thermal performance factors and heat transfer ratios due to enhanced effective thermal conductivity. Their analysis highlighted that maintaining low nanoparticle concentrations is essential to achieve heat transfer enhancement with acceptable pressure losses. Quantitatively, TiO_2 nanofluids at 0.5% concentration improved thermal rates by about 14.8%, while multi-walled carbon nanotube nanofluids at 0.6% yielded up to a 115% increase in heat transfer coefficient. Iron oxide nanofluids demonstrated a 41.29% rise in heat transfer rates with negligible pressure drop under magnetic field assistance, and hybrid Al_2O_3–TiO_2 nanofluids achieved up to 84% enhancement in thermal performance. Despite these promising outcomes, the authors emphasized the need for further studies on advanced surfactants, long-term stability, and comprehensive cost–benefit analyses to enable practical industrial adoption of nanofluid-based DPHE systems, while (Murthy *et al.* 2022) experimentally investigated the combined influence of water-based graphene oxide (GO) and Al_2O_3 nanofluids with propeller turbulator inserts in a counter-flow double-tube heat exchanger. With hot water flowing in the inner tube at Re = 2500 and nanofluids (0.05–0.15 vol.%) in the annulus at $500 \leq Re \leq 5000$, the maximum enhancement was achieved for 10 propellers and 0.15 vol.% Al_2O_3, yielding a 29.43% increase in Nusselt number and a thermal performance factor (TPF) of 1.32, accompanied by only a slight rise in friction factor. Empirical correlations for Nusselt number and friction factor were proposed, showing good predictive accuracy within −14% to +10% and −10% to +5%, respectively.

In addition to the overall heat transfer coefficient, parameters such as LMTD, NTU, effectiveness, capacity ratio, friction factor, and CHTC are critical for assessing the overall performance of a heat exchanger. Existing studies often focus on a limited subset of these parameters, frequently under a single nanoparticle concentration or flow condition. Moreover, only a few experimental investigations have systematically examined the combined influence of nanoparticle concentration and mass flow rate on these performance indicators in counter-flow double-tube heat exchangers. Recent studies have shown that while nanofluid addition enhances OHTC and CHTC, its effect on NTU, effectiveness, and pressure drop depends strongly on operating conditions (Rasheed *et al*. 2020; Reddy *et al.* 2025), highlighting the need for a balanced and integrated assessment. Based on these considerations, the present study provides a comprehensive experimental evaluation of Al_2O_3–water nanofluids in a counter-flow double-tube heat exchanger over a wide range of operating conditions. Nanofluids were prepared at four volume concentrations (0.01%, 0.1%, 0.2%, and 0.3%) and compared with the base fluid over mass flow rates ranging from 0.012 to 0.026 kg/s. The study systematically investigates the variation of Re, capacity ratio, LMTD, OHTC, NTU, friction factor, effectiveness, and CHTC. The results demonstrate that although nanoparticle addition slightly reduces Re due to increased viscosity, substantial enhancements in OHTC and CHTC are achieved. The nanofluids also exhibit higher NTU and effectiveness than the base fluid, confirming improved heat transfer performance with minimal hydraulic penalties. This work bridges existing research gaps by providing correlated experimental data encompassing both thermal and hydraulic characteristics of Al_2O_3–water nanofluids in a double-tube heat exchanger, contributing to the development of compact and energy-efficient thermal systems for renewable energy, electronic cooling, and advanced thermal management applications.

2. MATERIALS AND METHODS

2.1 Synthesis of Al_2O_3 Nanoparticles

Aluminium oxide nanoparticles were synthesized in the laboratory using a precipitation method, as shown in Fig. 1, to ensure high purity and uniform particle distribution. Analytical-grade aluminium nitrate nonahydrate ($Al(NO_3)_3 \cdot 9H_2O$) and ammonium hydroxide (NH_4OH) were used as precursors.

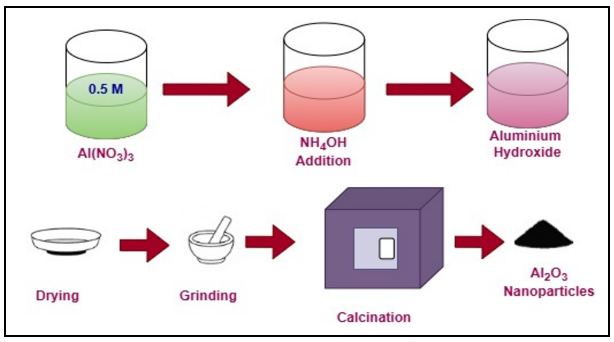


Fig. 1: Schematic representation of Al_2O_3 nanoparticle synthesis by chemical precipitation method

All chemicals were of Analytical Reagent (AR) grade and used without further purification. A 0.5 M aqueous solution of aluminium nitrate was prepared and continuously stirred using a magnetic stirrer at 400 rpm. Ammonium hydroxide ($Al(OH)_3$) solution (1 M) was then added dropwise until the pH of the solution reached approximately 9. The addition of the base resulted in the formation of a white gel-like precipitate of $Al(OH)_3$. The mixture was stirred for 2 hours to complete the precipitation process. The resulting precipitate was aged for 12 hours, filtered, and washed repeatedly with distilled water and ethanol to remove residual nitrate ions and impurities. The washed product was then dried in a hot-air oven at 100 °C for 10 hours to remove moisture. Then the dried powder was calcined in a muffle furnace at 600 °C for 3 hours to obtain crystalline Al_2O_3 nanoparticles. The calcined nanoparticles were lightly ground using an agate mortar to obtain a fine powder suitable for nanofluid preparation.

2.2 Preparation of Al_2O_3–water Nanofluids

The synthesized Al_2O_3 nanopowder was used to prepare nanofluids at volume concentrations of 0.01%, 0.1%, 0.2%, and 0.3%, along with a base-fluid sample (0%) for comparison. Distilled water was used as the base fluid because of its thermal stability and known physical properties. A two-step method was employed for nanofluid preparation. The required mass of Al_2O_3 nanoparticles for each concentration was calculated using the volume fraction relation. The measured nanoparticles were gradually added to the base fluid under constant stirring at 700 rpm for 60 minutes to obtain a uniform suspension. The mixture was then subjected to ultrasonic agitation using a probe-type ultrasonicator (20 kHz, 750 W) for 45 minutes to achieve uniform dispersion and minimize agglomeration. A small quantity (0.1 wt.%) of sodium dodecyl sulfate (SDS) was added as a surfactant to enhance the stability of the suspension. The prepared nanofluids were observed for sedimentation over 48 hours, showing excellent stability with no visible particle settling. All nanofluid samples were freshly prepared before each experimental run to ensure consistency.

2.3 Characterization of Al_2O_3 Nanoparticles

The morphology and surface characteristics of the synthesized Al_2O_3 nanoparticles were analyzed using Field Emission Scanning Electron Microscopy (FESEM) (Zeiss Sigma 300). The FESEM micrograph revealed quasi-spherical particles with a mean size distribution in the range of 40–60 nm and a tendency to form light agglomerates. The elemental composition was determined using Energy Dispersive X-ray Analysis (EDX) attached to the FESEM system. The EDX spectrum displayed characteristic peaks for aluminium (approximately 1.48 keV) and oxygen (approximately 0.52 keV), confirming the high purity of aluminium oxide and the absence of any metallic or foreign element contamination.

2.4 Experimental Setup and Procedure

A laboratory-scale double-pipe heat exchanger was designed and fabricated to investigate the thermal–hydraulic performance of Al_2O_3–water nanofluids under counter-current flow conditions. The experimental setup, shown schematically in Fig. 2(a) and photographically in Fig. 2(b), consists of a stainless-steel inner and outer tube assembly configured for counter-flow heat exchange.

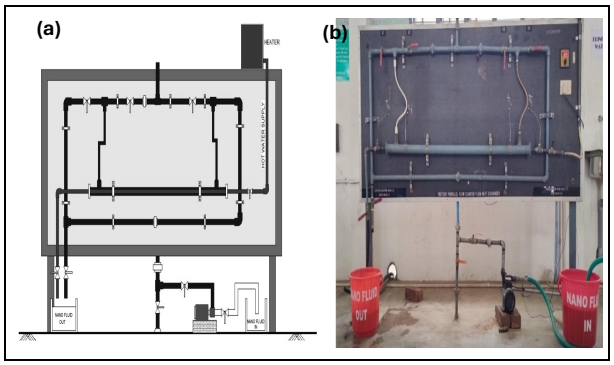


Fig. 2: (a) Schematic representation and (b) actual experimental setup of the double-tube heat exchanger test rig

The inner tube, through which the hot water flows, has an internal diameter of 12 mm, while the outer tube, carrying the cold nanofluid, has an inner diameter of 25 mm. The total effective length of the heat exchanger is 1 m. The annular and inner flow sections are insulated with a high-density thermal jacket to minimize heat loss to the surroundings. The hot water circuit includes a reservoir tank fitted with an electric heater, temperature controller, and magnetic stirrer to maintain a uniform inlet temperature of 67 ± 1 °C. The cold-fluid circuit consists of two reservoir tanks and a centrifugal pump that ensures continuous circulation of either the base fluid (distilled water) or Al_2O_3 nanofluid through the test section. Type-J thermocouples are installed at the inlet and outlet of both fluid streams to measure bulk temperatures, while precision rotameters are used to

regulate and measure the mass flow rates. The entire system operates under steady-state conditions, and data acquisition is performed using a digital multi-channel data logger. This experimental configuration enables a detailed investigation of how nanoparticle concentration and flow rate influence the convective heat transfer coefficient (CHTC) and related performance indicators such as the logarithmic mean temperature difference (LMTD), overall heat transfer coefficient (OHTC), number of transfer units (NTU), and heat exchanger effectiveness. The arrangement ensures reproducibility and allows for reliable comparison between the base fluid and nanofluid cases, thereby providing a comprehensive understanding of the influence of Al_2O_3 nanoparticles on heat transfer enhancement.

2.5 Measurement Uncertainty and Error Analysis

Measurement uncertainty and experimental errors were systematically evaluated to ensure the reliability and repeatability of the reported thermal–hydraulic results. All measuring instruments used in the experimental setup were calibrated before experimentation in accordance with standard laboratory procedures. Type-J thermocouples are used to measure inlet and outlet temperatures of the hot and cold fluids, with an accuracy of ±0.5 °C. Mass flow rates are measured using calibrated rotameters with an uncertainty of ±2% of the full-scale reading. Pressure drop across the test section is measured using a differential pressure gauge with an accuracy of ±1%. The geometric dimensions of the heat exchanger (tube length and diameters) are measured using a vernier caliper with an uncertainty of ±0.1 mm.

The uncertainties associated with derived parameters such as *Re*, LMTD, OHTC, CHTC, NTU, and effectiveness were estimated using the standard error propagation method. The combined uncertainty of a calculated parameter, R, which depends on multiple independent variables x_i, was determined using the root-sum-square method:

$$\left(\frac{\delta R}{R}\right) = \sqrt{\sum_{i=1}^{n} \left(\frac{\delta x_i}{x_i}\right)^2}$$

Based on this analysis, the maximum uncertainty in temperature measurement was ±0.8%, while the uncertainty in mass flow rate was within ±2%. The estimated overall uncertainty in calculated heat transfer coefficients (OHTC and CHTC) was found to be within ±5–7%, whereas the uncertainty in NTU and effectiveness was within ±6%. These uncertainty limits are considered acceptable for experimental heat transfer studies and are consistent with values reported in similar nanofluid-based heat exchanger investigations. The uncertainty analysis confirms that the observed enhancements in thermal performance using Al_2O_3–water nanofluids are significantly larger than the estimated experimental errors, thereby validating the reliability of the experimental results and conclusions drawn from the study.

2.6 Stability Assessment of Al_2O_3–water Nanofluids

The stability of the prepared Al_2O_3–water nanofluids was systematically assessed to ensure reliable thermal–hydraulic measurements. A stability duration of 48 h was selected to exceed the maximum continuous experimental run time and the total cumulative testing period for each nanofluid sample, thereby guaranteeing that sedimentation or agglomeration would not influence the measured results. Nanofluid stability was first evaluated through visual observation, where no visible sedimentation, phase separation, or particle clustering was detected over the 48-h period. To further enhance dispersion stability, a small amount of surfactant (0.1 wt.% SDS) was added, and probe ultrasonication was employed during preparation to minimize agglomeration and promote uniform particle distribution. In addition to visual inspection, the stability duration was selected based on commonly adopted practices in laboratory-scale nanofluid heat exchanger studies, where short-to-medium-term stability (24–72 h) is considered sufficient when nanofluids are freshly prepared and used immediately for controlled experiments. Since the present investigation focuses on steady-state thermal–hydraulic performance rather than long-term storage, the 48-h assessment was deemed appropriate and experimentally relevant. The observed stability indicates that the interparticle forces were effectively counterbalanced by electrostatic repulsion and steric effects introduced by the surfactant, ensuring consistent thermophysical properties throughout the testing period. Therefore, the chosen stability duration is adequate to support the validity, repeatability, and reliability of the experimental results reported in this study.

3. RESULTS AND DISCUSSION

3.1 X-ray Diffraction (XRD) and Fourier-Transform Infrared Spectroscopy (FTIR) Analysis of Al_2O_3 Nanoparticles

The crystalline structure and phase composition of the synthesized Al_2O_3 nanoparticles were analyzed using XRD, while FTIR spectroscopy was used to identify the functional groups and bonding characteristics. The corresponding XRD and FTIR spectra are shown in Fig. 3(a) and Fig. 3(b), respectively.

3.1.1 XRD Analysis

The XRD pattern of the synthesized Al_2O_3 nanoparticles, presented in Fig. 3(a), exhibits a series of sharp and well-defined diffraction peaks located at 2θ values of approximately 25.5°, 32.9°, 37.7°, 39.5°, 46.1°, 52.7°, 57.6°, 66.5°, and 77.1°, corresponding to the crystallographic planes (012), (014), (113), (116), (024), (018), (214), (300), and (1010). These reflections are in good agreement with the standard diffraction data for γ–Al_2O_3 (JCPDS card No. 10-0425), confirming the formation of a polycrystalline γ-phase aluminium oxide structure. The intense and narrow peaks indicate that the nanoparticles are well-crystallized. No additional impurity peaks were observed, verifying the high phase purity of the synthesized sample. The average crystallite size (D) of the Al_2O_3 nanoparticles was calculated using Scherrer's equation:

$$D = \frac{K\lambda}{\beta \cos\theta} \quad \ldots (1)$$

where, $K$is the shape factor (0.9), λ is the X-ray wavelength (1.5406 Å for Cu Kα radiation), β is the full width at half maximum (FWHM) of the most intense peak, and θ is the Bragg diffraction angle. The calculated average crystallite size was approximately 40–45 nm, which aligns well with the FESEM observations. The absence of secondary phases such as $Al(OH)_3$ or AlOOH suggests complete thermal decomposition of the hydroxide precursor during calcination at 600 °C, leading to the formation of pure γ–Al_2O_3 nanoparticles (Tan *et al.* 2024).

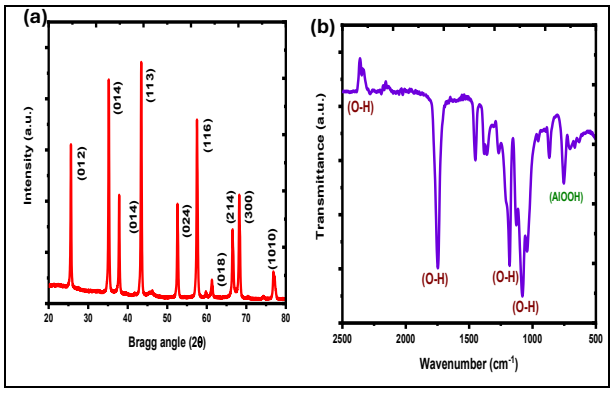


Fig. 3: (a) XRD and (b) FTIR spectra of synthesized Al_2O_3 nanoparticles

3.1.2 FTIR Spectroscopy Analysis

The FTIR spectrum of the synthesized Al_2O_3 nanoparticles is shown in Fig. 3(b). The characteristic absorption bands observed confirm the presence of functional groups associated with aluminium oxide. A broad absorption band centered around 3400 cm^{-1} corresponds to the O–H stretching vibrations, which can be attributed to adsorbed water molecules and surface hydroxyl groups on the nanoparticle surface. Additional weak bands observed near 1630 cm^{-1} are due to the bending vibrations of H–O–H groups from residual moisture. Strong absorption peaks in the lower wavenumber region, between 700 cm^{-1} and 500 cm^{-1}, are assigned to Al–O stretching and Al–O–Al lattice vibrations, which are the fingerprint features of aluminium oxide. A minor band around 1070 cm^{-1} corresponds to the AlOOH (boehmite) vibration mode, indicating trace hydroxide content, which is typical for Al_2O_3 nanoparticles synthesized via precipitation and low-temperature calcination. The FTIR results confirm the successful formation of Al–O bonds and the partial hydroxylation of the surface, consistent with the γ–phase aluminium oxide identified through the XRD analysis. The combination of XRD and FTIR findings thus validates the synthesis of pure, crystalline, and phase-stable Al_2O_3 nanoparticles with surface hydroxyl groups beneficial for stable dispersion in aqueous nanofluids (Yepuri *et al.* 2024).

3.2 FESEM and EDX Analysis of Al_2O_3 Nanoparticles

The surface morphology and elemental composition of the synthesized Al_2O_3 nanoparticles were examined using FESEM and EDX spectroscopy. The corresponding FESEM micrograph and EDX spectrum are presented in Fig. 4 (a) and Fig. (b), respectively.

3.2.1 FESEM Analysis

The FESEM image, shown in Fig. 4 (a), reveals that the synthesized Al_2O_3 nanoparticles are quasi-spherical and relatively uniformly distributed, forming loosely agglomerated clusters. The particles exhibit a flocculent or cauliflower-like morphology, which is characteristic of metal oxide nanoparticles synthesized via precipitation followed by calcination. Such agglomeration arises primarily from the high surface energy and van der Waals interactions between ultrafine particles. The observed particle size lies in the range of 40–60 nm, which is consistent with the crystallite size estimated from XRD analysis. Although particle agglomeration can influence nanofluid stability and rheological behavior by increasing the effective hydrodynamic diameter and viscosity, the agglomerates observed in the present study are non-compact and weakly bonded. These agglomerates can be effectively disrupted during nanofluid preparation through probe ultrasonication and surfactant addition, resulting in stable suspensions during experimental operation. At higher magnification, the formation of interconnected nanoparticle networks is evident, which enhances the available surface area and promotes micro-convection and localized heat transfer when dispersed in the base fluid. The well-defined granular morphology and limited grain growth during calcination confirm the successful synthesis of nanosized Al_2O_3 suitable for nanofluid-based heat exchanger applications, where the thermal performance benefits outweigh the modest viscosity-induced hydraulic penalties.

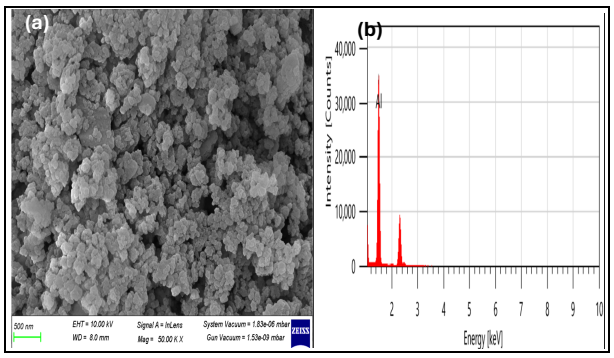


Fig. 4: (a) FESEM image and (b) the corresponding EDX spectrum of synthesized Al_2O_3 nanoparticles

The EDX spectrum, shown in Fig. 4 (b), displays prominent peaks corresponding to aluminium (Al) and oxygen (O) elements. The strong Al peak appears near 1.48 keV, and the O peak occurs around 0.52 keV, confirming the presence of aluminium oxide as the major component. The absence of any additional peaks indicates that the synthesized nanoparticles are free from impurities or residual precursor elements, validating the chemical purity of the sample. Quantitative EDX analysis confirmed an atomic ratio close to 2:3 (Al:O), which matches the stoichiometric composition of Al_2O_3. The high purity and elemental homogeneity observed in EDX complement the XRD results, verifying the successful synthesis of phase-pure γ–Al_2O_3 nanoparticles suitable for heat transfer applications.

3.3 Variation of Reynolds Number and Capacity Ratio

The variation of Reynolds number and Capacity ratio with mass flow rate for the base fluid and Al_2O_3 nanofluids is illustrated in Fig. 5(a) and Fig. 5(b), respectively. The analysis was conducted for different nanoparticle volume concentrations (0%, 0.01%, 0.1%, 0.2%, and 0.3%) over a mass flow rate range of 0.012–0.026 kg/s.

3.3.1 Reynolds Number

As shown in Fig. 5(a), Reynolds number (Re) increases linearly with mass flow rate for both the base fluid and the nanofluid. However, for each flow rate, the Reynolds number of the nanofluid is slightly lower than that of the base fluid. This reduction is primarily due to the increase in effective viscosity resulting from the addition of Al_2O_3 nanoparticles, which enhances intermolecular resistance to flow. The denser particle network within the fluid slightly retards motion, leading to a decrease in fluid velocity at a constant pumping power. The observed trend is consistent with classical nanofluid flow behavior, where the viscosity increase dominates over the small rise in density, resulting in a net decrease in Re at a fixed flow rate. Despite this reduction, all Reynolds number measurements fall within the laminar-to-transitional regime, ensuring that the effect of nanoparticle loading on hydrodynamic behavior remains moderate. The linear nature of the trend also confirms that the flow characteristics are stable and not influenced by particle clustering or sedimentation. Thus, the Reynolds number variation verifies the uniform dispersion of nanoparticles and the predictable flow dynamics of Al_2O_3 nanofluids inside the double-tube configuration.

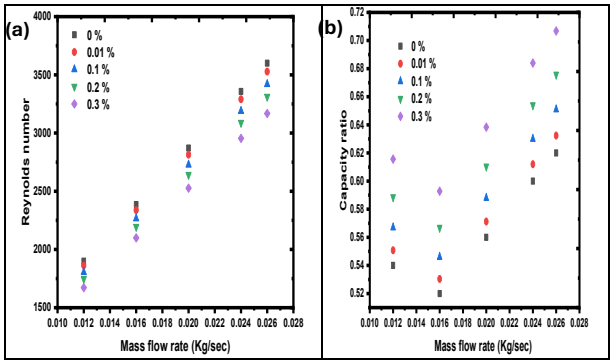


Fig. 5: (a) Reynolds number and (b) capacity ratio plotted against mass flow rate for the base fluid and Al_2O_3 nanofluids at various volume fractions

3.3.2 Capacity Ratio

Capacity ratio (C_r), the ratio of the minimum to maximum heat capacity rates of the two fluids, is an important non-dimensional parameter that governs the temperature driving potential in a heat exchanger. The variation of C_r with mass flow rate is shown in Fig. 5(b). At lower flow rates, a minor reduction in capacity ratio is observed for both the base fluid and the nanofluid, attributed to reduced heat-carrying capacity and higher temperature differentials between the streams. As the mass flow rate increases, the capacity ratio rises sharply and tends toward unity, indicating a more balanced thermal energy exchange between the hot and cold fluids. The addition of Al_2O_3 nanoparticles enhances the specific heat and thermal conductivity of the working fluid, resulting in a higher heat capacity rate compared to the base fluid. Consequently, the nanofluid exhibits slightly higher C_r values across all flow rates. The improvement becomes more pronounced at higher concentrations and mass flow rates, demonstrating the positive influence of nanoparticles on the energy storage and transport ability of the working fluid. Overall, the capacity ratio results confirm that the incorporation of Al_2O_3 nanoparticles leads to a thermodynamically favorable balance between the hot and cold fluid streams, contributing to enhanced heat transfer performance in the double-tube heat exchanger.

3.4. Variation of LMTD and OHTC

The variations of LMTD and OHTC with mass flow rate for the base and Al_2O_3 nanofluids are shown in

Fig. 6(a) and Fig. 6(b), respectively. These parameters were evaluated to assess the influence of nanoparticle concentration and flow rate on the overall thermal performance of the double-tube heat exchanger.

3.4.1 LMTD

As illustrated in Fig. 6(a), the logarithmic mean temperature difference (LMTD) is determined solely by the inlet and outlet temperatures of the hot and cold streams and therefore represents the thermodynamic temperature driving force for heat exchange rather than the intrinsic heat transfer capability of the working fluid. As the mass flow rate increases, the residence time of both fluids within the heat exchanger decreases, leading to smaller temperature changes between inlet and outlet conditions. This reduction in temperature difference consequently results in a gradual decrease in the calculated LMTD. The addition of Al_2O_3 nanoparticles does not directly enhance the LMTD. Instead, improvements in thermal conductivity and convective transport slightly modify the outlet temperatures, producing only minor variations in the computed LMTD values. Hence, LMTD should not be considered an indicator of heat transfer enhancement; rather, it reflects the available thermal driving potential, whereas parameters such as the overall heat transfer coefficient, NTU, and effectiveness more appropriately quantify the actual performance improvement of the heat exchanger.

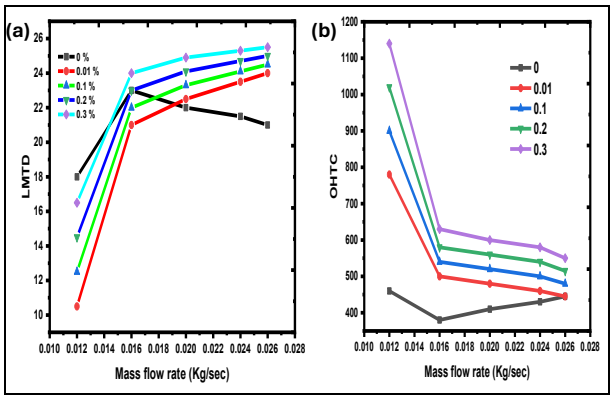


Fig. 6: (a) Variation of LMTD and (b) OHTC with mass flow rate for the base fluid and Al_2O_3 nanofluids

3.4.2 Overall Heat Transfer Coefficient (OHTC)

As shown in Fig. 6(b), the overall heat transfer coefficient (OHTC) increases with increasing mass flow rate for both the base fluid and the Al_2O_3 nanofluids. This increase is primarily attributed to higher fluid velocity, which reduces the thermal boundary layer thickness and enhances convective heat transfer. For all operating conditions, the nanofluids exhibit consistently higher OHTC values than the base fluid. The improvement arises mainly from the enhanced effective thermal conductivity and improved microscopic energy transport characteristics of the suspension, which reduce the overall thermal resistance of the system. The OHTC increases rapidly within the lower mass flow rate range (0.012–0.016 kg/s) and gradually approaches a plateau at higher flow rates, indicating diminishing incremental gains as convective resistance becomes less dominant. Consequently, the relative benefit of nanoparticle addition is more noticeable in the laminar and early transitional regimes, where improvements in thermophysical properties have a stronger influence on overall heat transfer performance.

The improvement in OHTC for the nanofluid is primarily due to three key factors:

- Enhanced effective thermal conductivity of the nanofluid, which facilitates faster heat transport between the tube wall and the bulk fluid;
- Particle migration and micro-convection, where random Brownian motion and localized eddies generated by nanoparticles increase mixing intensity near the boundary layer; and
- Improved surface wettability and reduced thermal boundary resistance, caused by the presence of oxide nanoparticles, which enhance wall-fluid thermal contact.

At higher mass flow rates, the rate of OHTC improvement becomes less significant because the thermal boundary layer becomes thinner, and the residence time decreases. Nevertheless, the nanofluids consistently exhibit higher OHTC values than the base fluid across the entire range of operating conditions, demonstrating superior thermal transport performance. The maximum enhancement in OHTC achieved at 0.3 vol.% nanoparticle concentration was approximately 25–30% higher than that of the base fluid, confirming the substantial potential of Al_2O_3 nanofluids for compact heat exchanger applications.

3.5 Variation of NTU and Friction Factor

The variation of the NTU and friction factor, *f*, with mass flow rate for the base fluid and Al_2O_3–water nanofluids is presented in Fig. 7(a) and Fig. 7(b), respectively. These parameters provide key insights into the overall thermal effectiveness and hydraulic performance of the double-tube heat exchanger.

3.5.1 NTU

As shown in Fig. 7(a), the NTU values are significantly higher for the Al_2O_3 nanofluids compared to the base fluid across all mass flow rates. At low flow rates (0.012 kg/s), the NTU of the nanofluid is nearly 1.5–1.7 times greater than that of the base fluid, indicating superior heat transfer performance. This enhancement is mainly attributed to the increase in convective heat transfer coefficient and effective thermal conductivity

due to the suspended nanoparticles. At low flow rates, the longer residence time of the working fluid inside the heat exchanger allows more effective thermal interaction between the hot and cold streams. The presence of nanoparticles further facilitates energy exchange by disrupting the boundary layer and promoting micro-scale convection. As the mass flow rate increases, the NTU gradually decreases for both fluids. This reduction is caused by the shorter residence time, which limits the amount of heat absorbed by the cold fluid per unit mass.

Despite the decrease with higher flow rates, the NTU of the nanofluid consistently remains above that of the base fluid, confirming that the Al_2O_3 nanoparticles enhance heat exchanger effectiveness even under high-throughput conditions. The higher NTU values for nanofluids suggest that the system can achieve the same thermal performance with a smaller heat exchanger size, demonstrating the potential of nanofluids for compact thermal management applications.

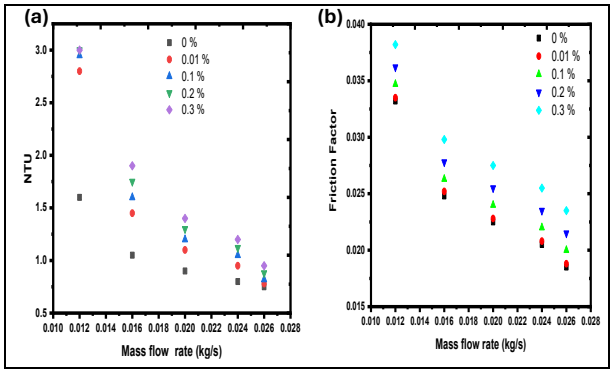


Fig. 7: Variation of (a) NTU and (b) friction factor with mass flow rate for the base and Al_2O_3 nanofluids

3.5.2 Friction Factor

The variation of the friction factor with mass flow rate is depicted in Fig. 7(b). For both the base fluid and the nanofluid, *f* decreases with increasing mass flow rate, a typical trend in internal flow systems. This inverse relationship is attributed to the transition from laminar to turbulent flow regimes and the corresponding reduction in relative viscous effects at higher velocities. The addition of Al_2O_3 nanoparticles leads to a slight increase in the friction factor compared to the base fluid. This increase is primarily due to the elevated viscosity and interparticle interactions that enhance the shear resistance at the wall. However, the magnitude of this increase remains modest within 5-10% for the highest nanoparticle concentration (0.3 vol.%), which is acceptable considering the substantial improvement in heat transfer performance. At higher flow rates, the difference in friction factor between the base fluid and nanofluid becomes negligible, suggesting that the viscosity effect diminishes as inertial forces dominate. Importantly, no unstable flow or excessive pressure drop was observed during the experiments, confirming that Al_2O_3 nanofluid maintains good flow stability and manageable pumping requirements throughout the tested range.

3.6 Variation of Effectiveness and CHTC

The variation of ε and CHTC with mass flow rate for the base fluid and Al_2O_3 water nanofluids is illustrated in Fig. 8(a) and Fig. 8(b), respectively. These parameters are critical indicators of the overall thermal performance and energy conversion efficiency of the double-tube heat exchanger.

3.6.1 Effectiveness (ε)

As shown in Fig. 8(a), the effectiveness of the double-tube heat exchanger decreases gradually with increasing mass flow rate for both the base fluid and the nanofluid. At lower flow rates (0.012–0.016 kg/s), the effectiveness is highest because the fluid has a longer residence time inside the heat exchanger, allowing a greater proportion of heat to be transferred between the hot and cold streams. As the mass flow rate increases, the contact time between the two fluids decreases, leading to reduced temperature differences and consequently lower effectiveness. Across all flow conditions, the Al_2O_3 nanofluids exhibit higher effectiveness values compared to the base fluid. The improvement in effectiveness becomes more prominent with increasing nanoparticle concentration. This enhancement can be attributed to:

- The increase in thermal conductivity of the working fluid, which facilitates faster heat diffusion across the thermal boundary layer;
- The improvement in the overall heat transfer coefficient (OHTC) due to particle-induced turbulence and micro-convective effects; and
- The reduction in thermal resistance at the solid–liquid interface caused by the presence of highly conductive Al_2O_3 nanoparticles.

At a 0.3 vol.% concentration, the effectiveness of the nanofluid was approximately 20–25% higher than that of the base fluid under identical flow conditions. This indicates that the Al_2O_3 nanofluid enables more efficient utilization of the available heat transfer surface area, making it a promising working fluid for compact and energy-efficient thermal systems.

3.6.2 CHTC

The variation of CHTC with mass flow rate is depicted in Fig. 8(b). For both the base fluid and the nanofluids, the CHTC increases steadily with increasing mass flow rate due to the higher flow velocity and reduced thermal boundary layer thickness. The convective mechanism becomes more dominant at elevated flow rates, resulting in improved heat transfer between the tube wall and the working fluid.

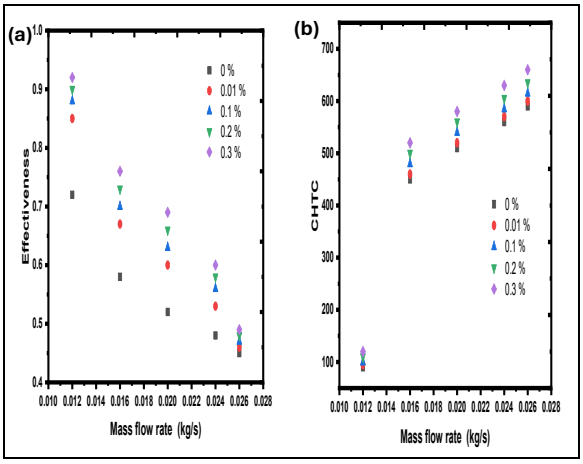


Fig. 8: Variations of (a) ε and (b) CHTC with mass flow rate for the base and Al_2O_3 nanofluids

The addition of Al_2O_3 nanoparticles significantly enhances the CHTC across all mass flow rates. The enhancement is primarily caused by:

- The increase in effective thermal conductivity of the fluid, which improves energy diffusion capacity;
- Micro-convection effects generated by Brownian motion and localized mixing of nanoparticles near the wall region; and
- The increased surface area of nanoparticles, which provides additional pathways for heat exchange between the fluid and the wall.

At the highest nanoparticle concentration (0.3 vol.%), the CHTC of the nanofluid was found to be approximately 30–35% higher than that of the base fluid. The improvement is more pronounced at lower flow rates, where the contribution of Brownian motion and particle–fluid interaction dominates, while at higher flow rates, the enhancement primarily arises from improved convective mechanisms. The results demonstrate that incorporating Al_2O_3 nanoparticles substantially strengthens the convective heat transfer characteristics of the system without imposing a significant hydraulic penalty, confirming the superior thermal–hydraulic performance of Al_2O_3–water nanofluids.

3.6.3 Pumping Power Analysis

To assess the hydraulic penalty associated with the use of Al_2O_3–water nanofluids, the pumping power requirement was evaluated and compared with that of the base fluid. The pumping power P_p was calculated using the following relation:

$$P_p = \Delta P \times Q$$

where, ΔP is the measured pressure drop across the test section and Q is the volumetric flow rate of the working fluid. The results indicate that the pumping power increases slightly with increasing nanoparticle concentration, which is consistent with the observed rise in friction factor and effective viscosity of the nanofluids. At the highest concentration of 0.3 vol.%, the increase in pumping power was found to be within 6–12% compared to the base fluid over the investigated mass flow rate range. This increase remains relatively small due to the moderate viscosity enhancement and stable flow behavior of the nanofluids.

Importantly, the modest increase in pumping power is significantly outweighed by the substantial improvement in thermal performance, with enhancements of approximately 25–30% in OHTC and 30–35% in CHTC. These results demonstrate a favorable trade-off between thermal gain and hydraulic penalty, confirming that Al_2O_3–water nanofluids can be employed effectively in double-tube heat exchangers without incurring excessive energy consumption for fluid circulation. The pumping power analysis, therefore, supports the practical applicability of the proposed nanofluid system for compact and energy-efficient heat exchanger applications.

4. CONCLUSION

This study experimentally investigated the thermal–hydraulic performance of a counter-flow double-tube heat exchanger using Al_2O_3–water nanofluids at different nanoparticle concentrations (0.01%, 0.1%, 0.2%, and 0.3% by volume) and mass flow rates (0.012–0.026 kg/s). The synthesized aluminium oxide nanoparticles were characterized using XRD, FTIR, FESEM, and EDX analyses, confirming the formation of pure γ–Al_2O_3 with nanoscale crystallinity and high phase purity. The structural and morphological characteristics contributed directly to the enhanced heat transfer capability of the prepared nanofluids.

The experimental outcomes can be summarized as follows:

- **Flow Behavior:**
  Reynolds number (Re) increased linearly with mass flow rate for all fluids, while it decreased slightly with nanoparticle addition due to an increase in viscosity. The flow regime remained within the laminar-to-transitional range, ensuring stable hydrodynamic behavior of the nanofluids.
- **Thermal Capacity:**
  The capacity ratio (C_r) increased with mass flow rate, and higher values were recorded for nanofluids compared to the base fluid. The improved heat capacity is attributed to the

enhanced specific heat and energy storage ability imparted by Al_2O_3 nanoparticles.

- **Temperature Driving Potential:**
The logarithmic mean temperature difference (LMTD) exhibited a gradual variation with flow rate, generally decreasing as the mass flow rate increased due to reduced residence time and smaller temperature differences between the inlet and outlet streams. Since LMTD represents only the thermodynamic temperature driving force for heat exchange, it is not a direct indicator of heat transfer enhancement. The addition of nanofluids caused only minor changes in the calculated LMTD values through slight modifications of outlet temperatures, while the actual improvement in thermal performance is more appropriately reflected by parameters such as the overall heat transfer coefficient, NTU, and effectiveness.

- **Overall Heat Transfer Performance:**
The overall heat transfer coefficient (OHTC) increased significantly with nanoparticle concentration and mass flow rate. The maximum OHTC enhancement reached approximately 25–30% at 0.3 vol.% concentration compared with the base fluid, demonstrating the strong influence of Al_2O_3 nanoparticles on overall heat transfer.

- **Energy Transfer Capability:**
The number of transfer units (NTU) increased notably for nanofluids, indicating enhanced heat exchanger effectiveness. The effectiveness (ε) values were also higher (up to 20–25% improvement at 0.3 vol.%), highlighting the superior energy conversion efficiency of the nanofluid system.

- **Convective Enhancement:**
The convective heat transfer coefficient (CHTC) showed the most substantial improvement, rising by approximately 30–35% over the base fluid. This enhancement is attributed to nanoparticle-induced micro-convection, increased surface area, and improved thermal diffusion near the tube wall.

- **Hydraulic Performance:**
The friction factor, *f,* increased marginally (by 5–10%) with nanoparticle addition, which remains within acceptable limits. The trade-off between enhanced heat transfer and minor pressure drop indicates that the system can operate efficiently without requiring excessive pumping power.

Overall, the incorporation of Al_2O_3 nanoparticles into water significantly enhanced the thermal conductivity, convective heat transfer performance, and energy transfer effectiveness of the double-tube heat exchanger, with only a minimal increase in hydraulic losses. An optimal nanofluid concentration of 0.2–0.3 vol.% was identified, providing the best trade-off between heat transfer enhancement and flow resistance. These results demonstrate the potential of Al_2O_3–water nanofluids as efficient working fluids for compact and energy-efficient heat exchangers used in refrigeration, thermal management, and renewable energy applications. Future work will focus on the long-term nanofluid stability and performance evaluation under extended operating conditions.

DATA AVAILABILITY STATEMENT

The datasets generated and/or analyzed during the current study are available from the corresponding author upon reasonable request.

FUNDING

This research received no specific grant from any funding agency in the public, commercial, or not-for-profit sectors.

CONFLICTS OF INTEREST

The authors declare that there is no conflict of interest.

COPYRIGHT

This article is an open-access article distributed under the terms and conditions of the Creative Commons Attribution (CC-BY) license (http://creativecommons.org/licenses/by/4.0/).



REFERENCES

Ajeeb, W., Thieleke da Silva, R. R. and Murshed, S. S., Experimental investigation of heat transfer performance of Al_2O_3 nanofluids in a compact plate heat exchanger, *Appl. Therm. Eng.*, 218, 119321 (2023). https://doi.org/10.1016/j.applthermaleng.2022.119321

Aldbea, F. W., Vázquez-Vázquez, C., Abobaker, M., Alsteeni, A., Saad, A., Sharma, A., Singh, P. K., Diantoro, M., May, M., Abdullah, T., Edhirej, A., Aldosari, S. and Kraini, M., Structural and optical properties of α-aluminum oxide prepared by sol–gel method, *Curr. Appl. Phys.*, 71, 85–90 (2025). https://doi.org/10.1016/j.cap.2024.12.008

Ayoob, H. W., Omar, I., Ghanim, W. K., Fares, M. N., Fazilati, M. A., Salahshour, S. and Esmaeili, S., Thermal–flow performance of water–Al_2O_3 nanofluid flow in an elliptical duct heat exchanger equipped with two rotating twisted tapes, *Case Stud. Chem. Environ. Eng.*, 11, 101094 (2025). https://doi.org/10.1016/j.cscee.2025.101094

Bashtani, I., Esfahani, J. A. and Kim, K. C., Effects of water–aluminum oxide nanofluid on double-pipe heat exchanger with gear disc turbulators: A numerical investigation, *J. Taiwan Inst. Chem. Eng.*, 124, 63–74 (2021). https://doi.org/10.1016/j.jtice.2021.05.001

Choi, S. U. S., Enhancing thermal conductivity of fluids with nanoparticles, *Proc. ASME Int. Mech. Eng. Congr. Expo.*, 66, 99–105 (1995). https://doi.org/10.1115/IMECE1995-0926

Das, L., Aslfattahi, N., Habib, K., Saidur, R., Das, A. and Kadirgama, K., Thermohydraulic performance investigation of a heat exchanger with combined effect of ribbed insert and Therminol-55/MXene+Al_2O_3 nanofluid: A numerical two-phase approach, *Heliyon*, 9(3), e14283 (2023). https://doi.org/10.1016/j.heliyon.2023.e14283

Ghazanfari, V., Imani, M., Shadman, M. M., Amini, Y. and Zahakifar, F., Numerical study on the thermal performance of shell-and-tube heat exchanger using twisted tubes and Al_2O_3 nanoparticles, *Prog. Nucl. Energy*, 155, 104526 (2022). https://doi.org/10.1016/j.pnucene.2022.104526

Ghazanfari, V., Taheri, A., Amini, Y. and Mansourzade, F., Enhancing heat transfer in a heat exchanger: CFD study of twisted tube and nanofluid (Al_2O_3, Cu, CuO, and TiO_2) effects, *Case Stud. Therm. Eng.*, 53, 103864 (2023). https://doi.org/10.1016/j.csite.2023.103864

Gkountas, A. A., Benos, L. T., Sofiadis, G. N. and Sarris, I. E., Printed-circuit heat exchanger performance using Al_2O_3–water nanofluid: Effect of nanoparticle interfacial layer, *Therm. Sci. Eng. Prog.*, 22, 100818 (2021). https://doi.org/10.1016/j.tsep.2020.100818

Issa, R. J., Review on thermophysical properties and Nusselt number behavior of Al_2O_3 nanofluids in heat exchangers, *J. Therm. Sci.*, 30, 418–431 (2021). https://doi.org/10.1007/s11630-021-1266-1

Kumar, P. G., Thangapandian, N., Vigneswaran, V., Vinothkumar, S., Mouli Prasanth, B., and Kim, S. C., Heat transfer, pressure drop and exergy analyses of a shot-peened tube heat exchanger using Al_2O_3 nanofluids for solar thermal applications, *Powder Technol.*, 401, 117299 (2022). https://doi.org/10.1016/j.powtec.2022.117299

Mohammed, H., Hasan, H. A. and Wahid, M., Heat transfer enhancement of nanofluids in a double-pipe heat exchanger with louvered strip inserts, *Int. Commun. Heat Mass Transf.*, 40, 36–46 (2012). https://doi.org/10.1016/j.icheatmasstransfer.2012.10.023

Murthy, H. M. S. and Hegde, R. N., Heat transfer studies on double-tube heat exchanger with combined effect of propeller insert and water-based GO and Al_2O_3 nanofluids, *Sādhanā*, 47, 143 (2022). https://doi.org/10.1007/s12046-022-01913-3

Nam, H. T., Lee, S., Kong, M. and Lee, S., Numerical study of flow and heat transfer characteristics of Al_2O_3 nanofluid in a double-pipe helical coil heat exchanger, *Micromachines*, 14(12), (2023). https://doi.org/10.3390/mi14122219

Patil, S. M., Radhakrishnan, A., Pawar, S. R., Railis, D. J. and Barmavatu, P., Prediction of heat exchanger efficiency in laminar swirling flow of graphene-oxide-based nanofluids using machine learning, *Numer. Heat Transf. Part B*, 86(12), 4149–4167 (2025). https://doi.org/10.1080/10407790.2024.2377792

Rashid, F. L., Al-Obaidi, M. A., Al-Maimuri, N. M. L., Abdalrahem, M. K., Ameen, A., Al-Munaf Ibrahim, O. A., Kadhim, S. A., Eleiwi, M. A. and Agyekum, E. B., Enhancing efficiency in double-pipe heat exchangers: A detailed review of nanofluids and their impact on thermal performance, *Heat Transf.*, 55(1), 212–240 (2025). https://doi.org/10.1002/htj.70070

Rasheed, A. H., Alias, H. B. and Salman, S. D., Experimental and numerical investigations of heat transfer enhancement in shell and helically microtube heat exchangers using nanofluids, *Int. J. Therm. Sci.*, 159, 106547 (2020). https://doi.org/10.1016/j.ijthermalsci.2020.106547

Reddy, G. S., Kalaivanan, R., Uday Kumar, R. and Jadhav, P. H., Influence of W-cut twisted tape inserts on heat transfer characteristics of a counter-flow heat exchanger using CeO_2 nanofluid: Experimental and numerical investigations, *Numer. Heat Transf. Part A*, 86(23), 8425–8445 (2025). https://doi.org/10.1080/10407782.2024.2359060

Tan, P., Liu, X., Liu, C., Feng, J. and Yang, K., Experimental study on heat transfer performance of a series-combined microchannel heat dissipation system using Al_2O_3 nanofluid, *Appl. Therm. Eng.*, 240, 122237 (2024). https://doi.org/10.1016/j.applthermaleng.2023.122237

Yepuri, V. and Ramachandramurthy, P., Impact of sol–gel synthesized α-aluminium oxide nanoparticles on transformer oil insulation properties, *Kuwait J. Sci.*, 52(1), 100331 (2024). https://doi.org/10.1016/j.kjs.2024.100331